Green way of improving the thermal efficiency of mortars by the addition of biobased phase change materials

Andrea Rubio-Aguinaga[1], *José María* Fernández[1], *Íñigo* Navarro-Blasco[1], and *José Ignacio* Álvarez[1*]

[1]MATCH Research Group, Department of Chemisty, School of Sciences, University of Navarra, C/. Irunlarrea 1, 31008 Pamplona, Spain

Abstract. The thermal efficiency of air lime-based mortars was improved by directly integrating varying amounts (5 wt. %, 10 wt. %, and 20 wt. %) of a microencapsulated biobased phase change material (PCM) into the fresh mortars. This PCM is made of vegetable oils and other organic wastes from the agri-food sector. The mortar formulation was optimized by adding different chemical additives and mineral admixtures. The mortar formulation was meticulously designed to produce rendering mortars that are easily workable, crack-free, and fully adherent for use in building envelopes. Positive outcomes in thermal efficiency tests have demonstrated the ability of these materials to store thermal latent energy, offering an environmentally friendly alternative to enhance the thermal comfort of building inhabitants.

1 Introduction

The enhancement of thermal efficiency in building materials has become imperative due to the substantial energy consumption associated with the construction sector, which contributes significantly to overall energy usage in Europe [1,2]. Heating and cooling of buildings, constituting a major portion of this consumption, heavily rely on fossil fuels, leading to greenhouse gas emissions. Therefore, improving the thermal comfort and efficiency of buildings has become primordial [3–7]. One viable solution to improve thermal efficiency and reduce energy demand is Thermal Energy Storage (TES). TES is achieved by heating, melting, vaporizing, cooling or solidifying a substance producing this way energy available as heat [5,7,8]. Among TES methods, Latent Heat Thermal Energy Storage (LHTES), also known as phase change materials (PCMs), stands out for its higher storage density and isothermal storage process [5,9–11].

A PCM can storage energy by absorbing heat as it undergoes endothermic phase changes as solid to solid, solid to liquid and liquid to gas and by releasing heat when exothermic processes take place such as solid to solid, gas to liquid and liquid to solid [3,12–14]. The

* Corresponding author: jalvarez@unav.es

These proceedings are published with the support of EuLA.

utilization of PCMs to enhance the thermal efficiency of construction materials is gaining popularity, and there have been several publications and research studies on the topic [7,11,14–19]. The achievement of thermal performance improvement using PCMs requires: a high phase transition latent heat per unit of volume, high thermal conductivity in both phases, small volume variation between the phase changes, high density, congruent melting, no supercooling, completely reversible transitions, low vapour pressure, high compatibility with building materials, no degradation in the operational temperature range, must be non-dangerous substances (non-flammable, non-toxic, non-explosive, non-corrosive…) and must be relatively economic and have a simple large scale production [5,12,20].

PCMs can be classified according to their phase change into four groups: gas-liquid, gas-solid, solid-liquid and solid-solid [5,12,14]. Although solid-gas and liquid-gas show higher enthalpies ascribed to the transitions the volume variation associated to those phase changes makes its application in building materials unfeasible [5,12,21]. On the other hand, solid-solid PCMs present the advantage of the maintenance of the shape during the phase changes but their main drawback is their low enthalpy values ascribed to that phase change [5,22]. Due to these reasons, the most widely used PCMs are liquid-solid since they have relatively high enthalpy of melting and their volume variation is not so limiting [1,12,22]. The principle of solid-liquid PCMs for improving the thermal performance of building materials is based on the absorption of heat when the material temperature is higher than the melting temperature (T_m) of the PCM, thus storing latent heat of fusion, and when the system temperature is lower than the T_m of the PCM, the previously absorbed heat is released through the exothermic process of solidification. Thus, depending on the external temperature, the PCM can absorb or release heat mitigating the differences between peak and off-peak thermal loads, reducing the energy consumption, cutting in electricity demand, improving the indoor thermal comfort, and, therefore, reducing the CO_2 emissions to the atmosphere [2,19,22].

Solid-liquid PCMs can be further classified according to their composition into organic compounds (paraffin waxes, fatty acids, sugar alcohols and crystalline polymers) , inorganic salts (eutectic salts, salt hydrates and molten salts) and metals (simple metals and alloys) [22]. One of the most widely used solid-liquid PCMs are the paraffin-based ones [1,23]; however, one of their major drawbacks is their origin and production. Paraffin [C_nH_{2n+2}] is a petroleum-based product produced by the refining of crude oil [24,25]. Consequently, employing paraffin-based PCMs for the enhancement of the thermal storage of building materials is not as green and clean as it may appear since it implies the indirect use of fossil fuels [20]. In order to emphasize the eco-friendly nature of the thermal efficiency improvement, bio-based PCMs are employed in this research. Bio-based PCMs offer an eco-friendlier alternative to the widely used paraffin-based ones. Commonly, bio-based PCMs are organic fatty acid esters derived from renewable and underutilized raw materials such as animal fats and vegetable oils (lauryl alcohol, butyl stearate, palmitic acid, myristic acid…) [2]. Enthalpy values, melting temperatures, thermal stabilities and large scale production capacities of the bio-based PCMs are similar to the paraffinic PCMs and make them a promising way of enhancement the TES in a greener way [2].

One aim of this work is the thermal efficiency improvement of air lime-based rendering mortars through the direct incorporation of different doses of a PCM with melting temperature of 29ºC composed of methyl ester from agricultural sources. A microencapsulated version of this PCM was selected in order to: i) maintain the macroscopic shape when the phase change occurs, ii) to avoid migration and leakage, iii) to increase the heat transfer area, and iv) to protect the core from the interaction and interference with the matrix [5,22,25]. In addition, the mortar composition was rigorously optimized to allow its application as a building envelope, studying its adherence, the crack formation and shrinkage in various substrates. The addition of the microencapsulated PCMs could lead to the

alteration of the fresh and hardened mortars' properties yielding an unworkable render with no real-life application. Here lies precisely the importance of a proper formulation of PCM-bearing mortars intended to be used as renders in building envelopes such as floors, walls, facades, ceilings... This aspect is not usually considered in the literature and it is one of the main objectives of this work: to design a PCM-containing mortar that is applicable as a render.

The formulation optimization was carried out by the simultaneous addition of: a polycarboxylate ether derivative -as a superplasticizer- to avoid an excess of mixing water and to achieve an adequate consistency of the fresh render, and a potato starch derivative for the adhesion enhancement and limit the crack formation. In order to optimize the formulation using these chemical additives, their compatibilities and interactions with the microcapsules of the PCM were previously studied within the lime matrix. This study facilitated streamlining and refining the formulation optimization process.

Once the renders formulations were optimized, fresh mortar properties, mechanical performance, microstructural studies and thermal performance were assessed.

2 Materials and methods

2.1 Materials

Air lime rendering mortars were formulated by combining hydrated calcitic air lime (CL-90-S) from Cal Industrial S.A. and a very fine calcitic sand (particle size of 0 to 1 mm) supplied by CTH. The binder-to-aggregate weight ratio was maintained at 21.7/78.3, while the mixing water content was set at 25 wt. % of the total mortar weight.

Various additives and mineral admixtures were incorporated to fine-tune the mix composition in order to achieve renders that are easy to work with, and exhibit optimal performance. A superplasticizer (MasterCast GT 205, a polycarboxylated ether derivative) was introduced to regulate the fluidity of the fresh renders, thereby avoiding excessive water addition. Different proportions of a starch derivative (Casaplast) were included to enhance adhesion.

A bio-based microencapsulated PCM with a melting temperature of 29℃ (denoted in the text as 29PCM) was used. PCM were directly incorporated into fresh air lime mortars during mixing in 5%, 10%, and 20% by weight of lime (bwol).

For comparison purposes, a PCM-free mortar (CTRL) was prepared as control samples.

2.2 Methods

2.2.1 Mortars preparation

To prepare the fresh mortars, air lime, sand, adhesion booster, 29PCM, and an initial percentage of superplasticizer (0.25% by weight of lime, bwol) were blended for 5 minutes using a solid additives mixer BL-8-CA (Lleal, S.A., Granollers, Spain) to achieve a homogeneous mix.

A fixed proportion of mixing water (25 wt.%) was then introduced to a Proeti ETI 26.0072 (Proeti, Madrid, Spain) mixer at a slow speed for 270 seconds. Superplasticizer was incorporated gradually at 0.25% bwol until appropriate fluidity was attained (as assessed by the flow table test [26]). For each render, the superplasticizer percentages (together with the adhesion booster) were adjusted until appropriate, adherent, and low-cracking renderings were attained, as described in a previous work [27].

For the hardened state examination, fresh mixes were moulded into cylindrical specimens with dimensions of 30 mm diameter and 40 mm height, and then cured under lab conditions (20 ℃ ± 0.5 ℃ and 60% ± 5% RH). These dimensions were chosen to optimize the sample preparation process and they are suitable for measuring the mechanical compression strengths.

2.2.2 Compatibility and interaction studies: particle size distribution and zeta potential

The study of interactions was carried out by particle size distribution analysis using laser diffraction with a Malvern Mastersizer instrument. The experiments were divided into two sets:

1) Suspensions containing 5% wt/wt PCM in water were prepared, with varying amounts of superplasticizer (0%, 0.50%, 0.75%, 1%, and 1.5% by weight of PCM) or starch derivative (0%, 0.25%, 0.50%, 0.75%, and 1% by weight of PCM). This experiment was aimed to explore the interaction between PCMs and these additives.
2) Another series of experiments involved suspensions comprising 5% wt/wt lime, 5% bwol (by weight of lime) of PCM, and varying amounts of superplasticizer (0%, 0.50%, 0.75%, 1%, and 1.5% bwol) or starch derivative (0%, 0.25%, 0.50%, 0.75%, and 1% bwol). This assay was conducted to investigate the interaction between the PCM-lime matrix and the superplasticizer and the adhesion booster.

Zeta-potential measurements were utilized to investigate the electrostatic forces, both repulsive and attractive, among particles, providing valuable insights into the stability of various PCM-bearing mixtures. These measurements were conducted using a ZetaProbe device from Colloidal Dynamics, employing the electro-acoustic technique. The experiments were organized into three sets:

1) Sequential addition of 1 mL of 5% wt/wt PCM suspensions in water to 5% wt/wt aqueous lime suspensions to examine the interaction between lime and PCMs.

2) Titration with 0.02M NaOH of 5% wt/wt PCM suspensions in water, varying superplasticizer (0%, 0.50%, 0.75%, 1%, and 1.5% by weight of PCM) or starch derivative (0.25%, 0.50%, 0.75%, and 1% by weight of PCM) to investigate the interactions of these chemical additives with PCMs as pH varies.

3) Titration of 5% wt/wt lime and 5% bwol (by weight of lime) of PCM with 1% wt/wt aqueous suspensions of superplasticizer or adhesion booster to assess the PCM-lime interactions with the chemical additives.

2.2.3 Fresh state tests

Multiple assessments were carried out to characterize the freshly prepared mortars. The flowability of the fresh mortars was determined using the flow table test, adhering to the UNE-EN 1015-3 standard [26]. Additionally, the mortar's density and the percentage of entrapped air were measured following the UNE-EN 1015-6 [28] and UNE-EN 1015-7 [29] standards, respectively. Water retention capacity was determined according to the Spanish standard [30]. Finally, the setting time was evaluated in accordance with the UNE-EN 1015-9 standard [31].

2.2.4 Microstructural assessment: scanning electronic microscopy and mercury intrusion porosimetry

Mercury intrusion porosimetry (MIP) was utilized to examine the porous structure of the rendering mortars, and thus to try and see the impact of integrating PCMs on the mortar microstructure. MIP analyses were carried out employing a Micromeritics AutoPore IV 9500 instrument, covering a pressure range from 0.0015 to 207 MPa, and focusing on cubic fragments of the mortars measuring approximately 1 cm on each side.

Microstructure analysis was additionally conducted through scanning electron microscopy (SEM) utilizing the COXEM EM-30N electron microscope. Elemental analysis was performed using a Quantax Compact30 EDS probe (Bruker), with data processing facilitated by Esprit Compact software. Sample conductivity enhancement was accomplished by applying a gold coating using a COXEM SPT-20 ion sputter.

2.2.5 Mechanical performance: compressive strength resistance

The hardened mortars' compressive strength was assessed utilizing a Frank/Controls 81565 press fitted with a Proeti ETI 26.0052 compressive breaking device. Testing was performed at breaking speeds ranging from 20 to 50 N/s, with intervals of 30 to 90 seconds. Measurements were taken at curing ages of 28, 91, 182, and 365 days. Three cylindrical specimens were utilized for each sample to guarantee precise and indicative outcomes.

2.2.6 Thermal behaviour: thermal conductivity and thermal efficiency

Thermal conductivity (λ) was measured using the FOX50 Heat Flow Meter by TA Instruments. This device utilizes two plaques, each controlled by separate Peltier cells, to create a temperature difference of 10°C, generating a thermal gradient for conductivity determination.

Measurements were taken on 55 mm diameter disks of rendering mortars with thicknesses of 10 mm and 20 mm at temperatures ranging from 5°C to 35°C. This allowed assessment of conductivity in solid and liquid states of the tested PCMs. Lime-based renders were cured for at least 28 days prior to measurement. Three disks of each render were tested to ensure reliability, and averages with standard deviations were calculated. Thickness-independent λ values were determined using equations 1 and 2, where Q_1 and Q_2 represent heat flow transducer signals, S_{cal} is a calibration factor, Δx_1 and Δx_2 are thicknesses of specimens, and 2R is the sum of thermal contact resistances. A lower λ value indicates slower heat conduction through the material.

$$Q_1 = \Delta T / [(\Delta x_1/\lambda) + 2R) S_{cal}] \quad (1)$$

$$Q_2 = \Delta T / [(\Delta x_2/\lambda) + 2R) S_{cal}] \quad (2)$$

Experiments to explore the thermal performance of mortars, at a laboratory scale, were conducted using hotbox models. These models consisted of four small flat mortar slabs (measuring 9 x 18 cm and thickness 2 cm), housed within a thermally insulated box crafted from expanded polystyrene (Fig. 1a). The walls were tightly sealed with high-temperature-resistant silicone to ensure heat transfer occurred solely through them, facilitating a comparison of different mortar efficiencies. These setups were placed inside a climatic chamber (Fig. 1b) and subjected to four temperature cycles ranging from -10ºC to 50ºC, mimicking extreme outdoor conditions. One box acted as a control without PCM, while the other contained a specific quantity of PCM. Three strategically positioned thermocouples

monitored temperatures within the chamber and each box continuously. This monitoring allowed the study of PCM-integrated mortar's heat absorption and release.

Temperature data was analysed using OriginLab software to compute temperature differentials (ΔT) between the control and PCM-containing hotboxes at each time point. Additionally, the integral of ΔT over time (eq.3) was calculated to estimate the amount of heat transferred in joules (J), representing total energy exchange within the system during the time interval [t_1, t_2].

$$Q = \int_{t1}^{t2} \Delta T(t)\, dt \qquad (3)$$

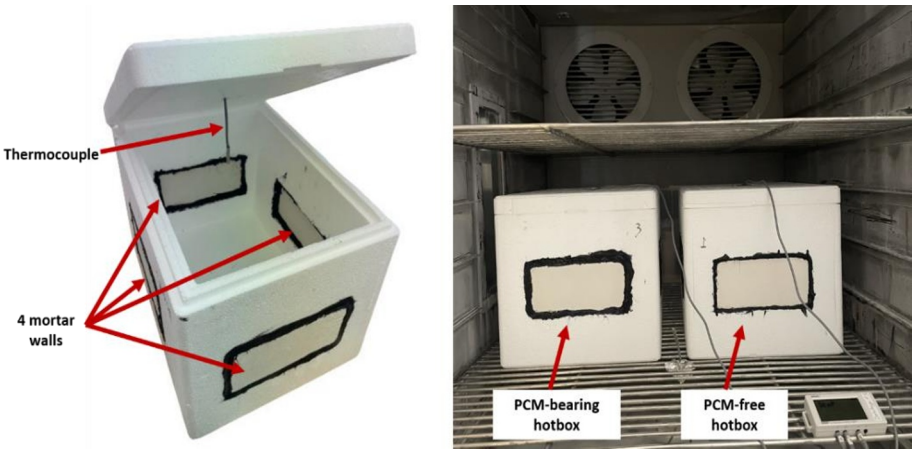

(a) (b)

Fig. 1. (a) hotbox and (b) arrangement of the hotbox experiment within the climatic chamber

3 Results

3.1.1 Compatibilities and interactions among the additives

In a preliminary stage, the compatibilities and interactions of different chemical additives, such as superplasticizer and adhesion booster, with the microencapsulated PCMs were investigated. This was achieved by analysing particle size distributions to assess the interactions between superplasticizer (SP) and 29PCM (Fig. 2a) and between the adhesion improver and 29PCM (Fig. 2b).

The results indicated that the particle size distribution remained unchanged with the addition of both superplasticizer (Fig. 2a) and adhesion booster (Fig. 2b), thus suggesting no direct interaction between the chemical additives and microencapsulated PCMs.

However, when lime was introduced into the system (Fig. 2 c-d), net effects on particle size distribution were observed. Increasing concentrations of superplasticizer in the 29PCM-lime system (Fig. 2c) led to a trend towards smaller particle sizes, highlighting the dispersing action that this additive exerts onto lime particles (deflocculating effect). Conversely, increasing the dosage of adhesion booster (Fig. 2d), generally resulted in a shift of the particle size distribution towards larger sizes, indicating the ability of this starch derivative to agglomerate lime particles.

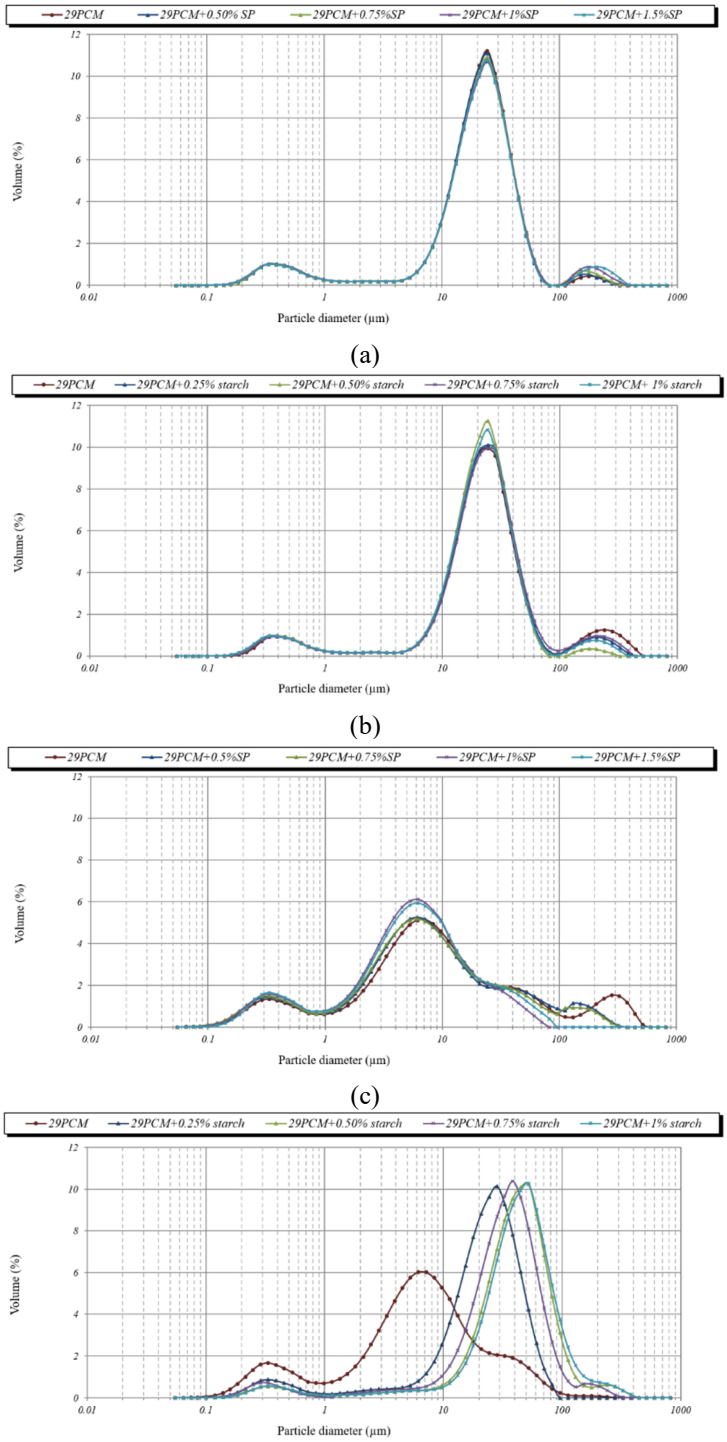

Fig. 2. Particle size distribution of: (a-b) 5% wt/wt 29PCM with increasing dosages of: (a) superplasticizer and (b) adhesion booster, (c-d) 5% wt/wt lime, 5% bwol of 29PCM with increasing dosages of: (c) superplasticizer and (d) adhesion booster.

The studies of interactions and compatibilities were complemented by the Z-potential experiments. In Figure 3a, the low interaction of 29PCM with any of the SP doses at any pH is observed with zeta potential values close to 0 mV. On the other hand, in Figure 3b, a more intense interaction of 29PCM with starch is evident. Partial adsorption of starch on the PCM could account for these more positive values of the zeta potential at the onset of titration. Afterwards, asymptotic values around 10 mV were attained for all doses, possibly due to interaction or agglomeration between particles, which hindered measurements across the entire surface of the microcapsules.

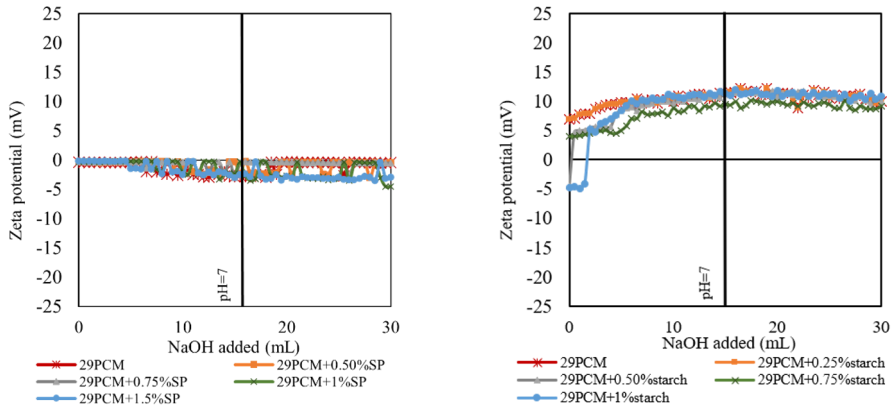

(a) (b)

Fig. 3. Zeta potential values of 0.02 M NaOH titration of 5% wt/wt 29PCM with either increasing dosages of: (a) superplasticiser and (b) starch.

Experiments involving 29PCM in a lime suspension demonstrated elevated positive zeta potential values (Fig. 4). Initially, the mortars, devoid of superplasticizer or adhesion booster, exhibited zeta potential values ranging from 80 to 90 mV due to the positive charge of the portlandite crystals [32]. Upon the introduction of both polymers, superplasticizer and starch, a notable increase in zeta potential was observed (up to 150–160 mV), followed by a gradual decline towards lower values. This trend is attributed to the formation of a second adsorption layer, as evidenced by previous studies [32]. In systems containing superplasticizer, the electrosteric dispersion phenomenon contributed to a lesser decrease in zeta potential. Conversely, in systems containing starch (Figure 5b), an agglomeration phenomenon prevailed, leading to a more pronounced reduction in zeta potential [33].

Therefore, based on the results, an indirect effect of the chemical additives on the PCM microcapsules, through the modification of the distribution of the lime particles, is observed.

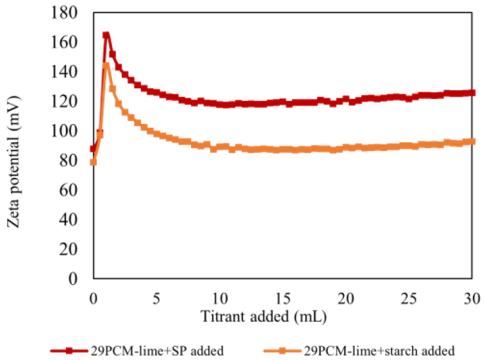

Fig. 4. Zeta potential values of 5 % wt/wt lime, 5% bwol 29PCM titrated with 1% wt/wt SP or 1% wt/wt starch.

3.1.2 Optimization of the formulation and fresh state tests

Once the interactions and compatibilities of the different additives present in the mortar were understood, formulation optimization was carried out. The dosages of superplasticizer and adhesion booster were adjusted for each percentage of 29PCM (5%, 10%, and 20%). In this way, it was possible to mitigate adverse effects, as reported in the literature, that manifest after the addition of PCMs such as reduced fluidity, crack formation, poor adhesion, etc. The optimized formulation, achieved after trial-and-error testing of different additive compositions, is presented in the Table 1. The good performance of the optimized renders is shown in Figure 5, once applied onto absorbent substrate. Single layers with thickness of 0.5 cm were applied onto half surface of saturated bricks and were kept covered for 15 days to prevent rapid drying of the mortars. All optimized mortars exhibit suitable consistencies for application as renders, being easily workable, crack-free, and adhering fully to the substrate.

Table 1. Optimised formulation of control renders (PCM-free) and 29PCM-bearing renders.

	CTRL	29PCM-5	29PCM-10	29PCM-20
PCM (% bwol)	0	5	10	20
SP (% bwol)	0.6	0.75	0.75	0.75
MK (% bwol)	0	0	0	0
Adhesion booster (% bwol)	0.50	0.50	0.50	0.50
Air lime (wt. %)	21.7	21.7	21.7	21.7
Calcitic sand (wt. %)	78.3	78.3	78.3	78.3
Water (wt. %)	25	25	25	25

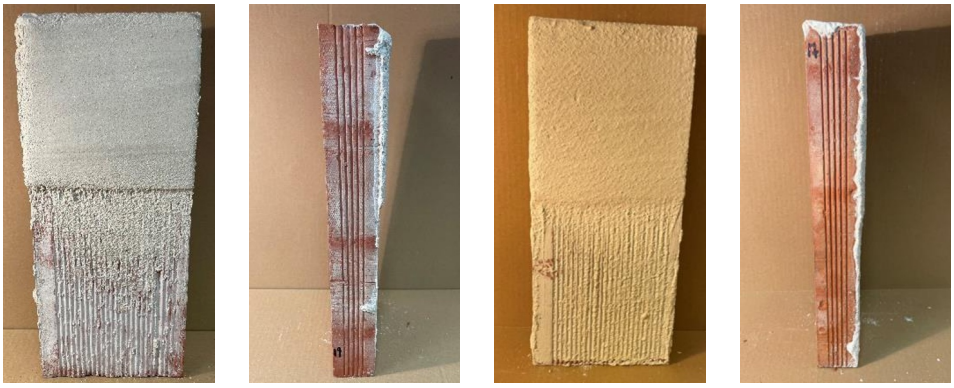

(a) (b) (c) (d)

Fig. 5. Rendering of mortar on saturated brick containing: (a,b) 0.50% starch, 0.75% SP and 5% 29PCM (frontal and side face) and (c,d) 0.50% starch, 0.75% SP, 10% 29PCM (frontal and side face).

The fresh characterization of the optimized mortars was conducted by studying consistence, stiffening time, mortar density, occluded air, and water retentivity (Table 2). It was observed that the only property that varies upon the addition of 29PCM is consistence, which generally increases after incorporating this additive. However, the workability and fluidity remain suitable for application as renders (Fig. 5). The other parameters, thanks to the formulation optimization, remain practically unchanged after the addition of 29PCM at any assayed percentage.

Table 2. Fresh state test results for optimised renders.

Sample	CTRL	29PCM-5	29PCM-10	29PCM-20
Consistence (mm)	182	179	190	214
Stiffening time (min)	1157	1397	1047	1277
Fresh mortar density (kg/m^3)	1940	1900	1890	1870
Occluded air (%)	4.3	4.3	5.2	6.0
Water retentivity (%)	95.9	96.9	93.7	92.7

3.1.3 Assessment of the microstructure of the hardened mortars

The microstructural characterization of the hardened mortars carried out with SEM revealed the attainment of homogeneous materials in which the microencapsulated PCMs were evenly distributed within the matrix (Figure 6). For the most part, the microcapsules remain intact without their integrity being compromised. In fact, it can be observed how the lime matrix perfectly accommodates these microcapsules, resulting in a complete integration of the PCMs into the mortar (Figure 6).

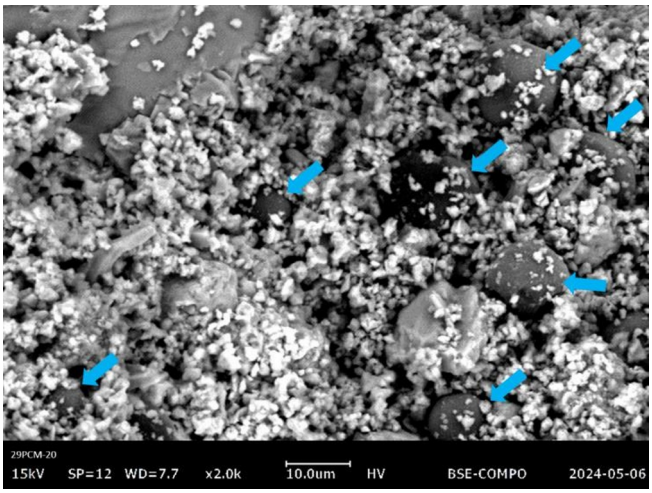

Fig. 6. SEM micrograph of 29PCM-20 render at 91 curing days. Blue arrows denote intact 29PCM microcapsules.

The microstructural characterization was complemented with MIP, the findings of which are documented in Figure 7. It can be seen how after the addition of the 29PCM the pore size distribution subtlety shifts to higher pore sizes (Figure 7a). Moreover, the incorporation of 29PCM led to an augmentation in the volume of intruded mercury, as indicated by the area under the curve (AUC). These results would thus indicate an increase in the porosity of the mortar after the addition of PCM.

The average pore size of the mortar containing 20% of 29PCM (29PCM-20) notably increases, an average of 30%, when compared with the control mortar (Figure 7b).

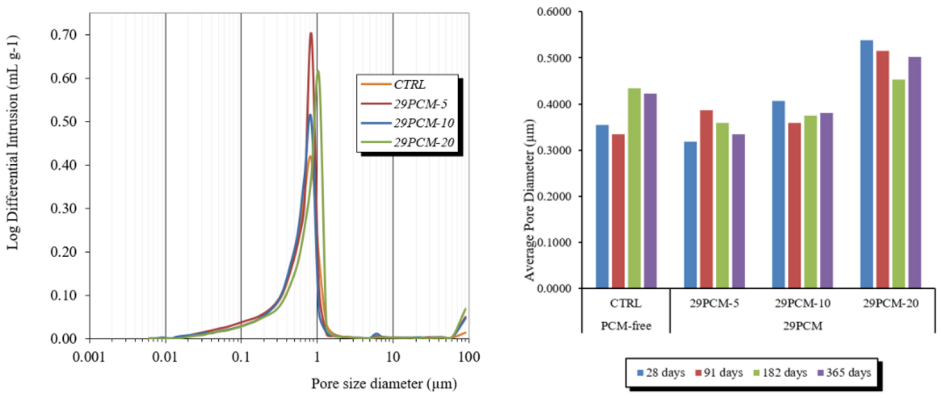

(a) (b)

Fig. 7. Pore size distributions of mortars at 91 curing days.

3.1.4 Mechanical strength

The mechanical performance of the mortars at curing ages of 28, 91, 128, and 365 days was evaluated. Comparing the PCM-free mortar with the 29PCM-bearing mortars, it can be observed that the addition of up to 10% of 29PCM results in an improvement in compressive strength (Figure 8). Only a deterioration in mechanical performance is observed with the highest dosage of 29PCM (20% bwol). This detriment in mechanical performance could be explained by the more drastic increase in mean pore size experienced by this mortar (29PCM-20).

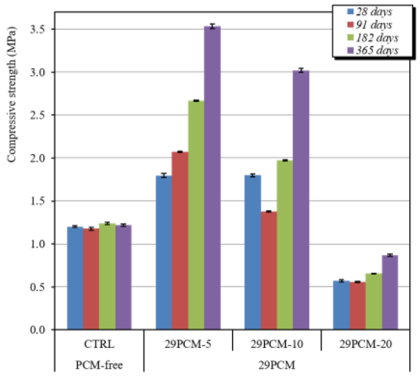

Fig. 8. Compressive strength measurements of the renders at various curing days.

3.1.5 Thermal performance evaluation

Concerning the thermal conductivity assessments, Figure 9 depicts the thickness-independent λ values obtained at 5°C, 15°C, 25°C, and 35°C. These temperatures were strategically selected for analysis: firstly, to investigate conductivity below the melting points of the two PCMs tested (5°C); secondly, to explore conductivity in proximity to these points (15°C and 25°C); and finally, to examine behaviour at temperatures notably higher than these points (35°C). Across all examined samples, the recorded thermal conductivity coefficients align with the typical range expected for such materials [34,35].

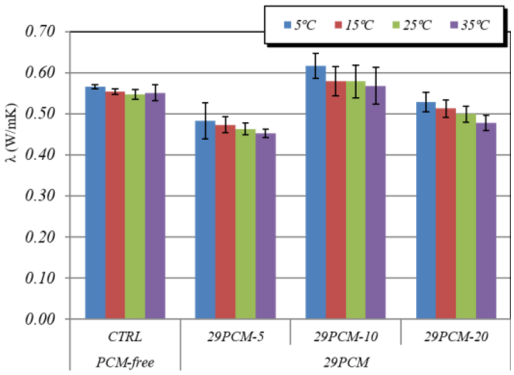

Fig. 9. λ values the at 5°C, 15°C, 25°C and 35°C.

The experiments conducted on PCM-bearing renders indicate that incorporating any dosage of 29PCM does not significantly impact the mortar's thermal conductivity. This fact is highly advantageous for practical application, as it ensures that heat can effectively permeate the material and reach the core of the PCM microcapsules during phase change melting and vice versa during solidification. Furthermore, a clear correlation between thermal conductivity (λ) values and temperature is evident: higher temperatures correspond to lower thermal conductivity. This trend can be attributed to the lower thermal conductivity of PCMs in their liquid state compared with their solid state, a phenomenon consistent with findings in existing literature [25].

The evaluation of the thermal energy efficiency of lime rendering mortars involved conducting hotbox experiments to assess their thermal storage and release capabilities. Figure 10a illustrates the temperature variations during heating-cooling cycles. The graph shows the temperatures of both the climatic chamber and the interior of the hotboxes under test. During the heating phase, 29PCM-bearing mortars absorb heat as the PCMs melt, thereby lowering the temperature inside the hotbox (Figure 10b). Conversely, during the cooling phase, the PCMs release stored heat as they solidify, raising the ambient temperature within the hotbox (Figure 10c). These effects simulate real-world applications where buildings treated with such renderings could better regulate internal temperatures, resulting in reduced cooling and heating expenses. The evaluation of thermal efficiency throughout the entire cycle was performed by integrating the temperature fluctuations compared with the reference (mortar without PCMs, CTRL) over time. This approach allows for the calculation of the energy or heat exchanged during cold-heat cycles, providing a measure of the actual capability of PCMs to enhance thermal comfort. Table 3 gathers the energy exchanged for each 29PCM-bearing mortar.

Table 3. Energy exchanged calculated by the integral of the temperature variation *vs* time

Render	PCM (% bwol)	Energy exchanged (kJ/m^2)
29PCM-5	5	420
29PCM-10	10	440
29PCM-20	20	710

The exchanged energy values indicate a high attenuation of temperatures by the 29PCM over the complete heating and cooling cycles. These results demonstrate the ability of the biobased 29PCM to increase thermal comfort, as they effectively smooth temperatures through the release/absorption of latent heat ascribed to phase changes. Furthermore, it has been shown that with a very small amount of this additive (the mortars tested contained 0.01-

0.04 g of 29PCM per gram of dry mortar) a remarkable improvement in thermal efficiency is possible.

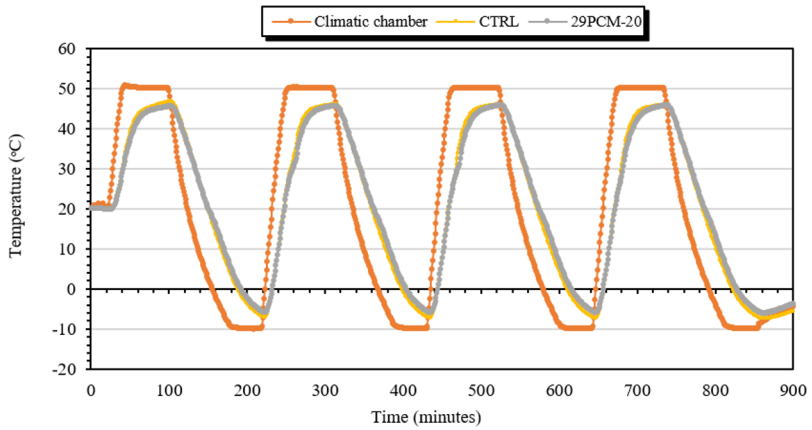

(a)

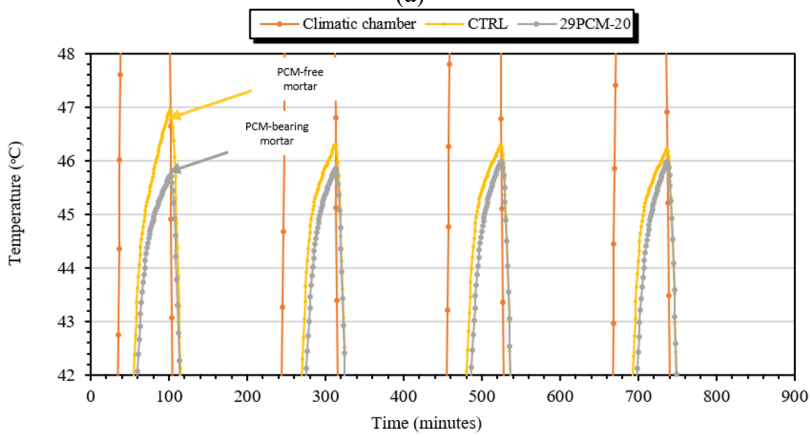

(b)

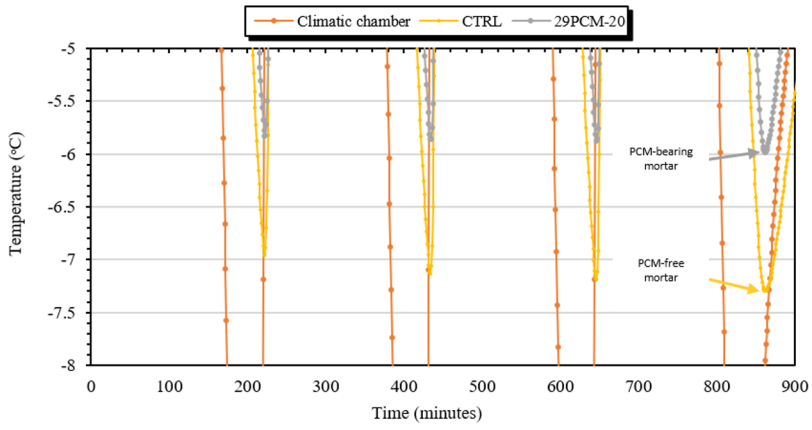

(c)

Fig. 10. Energy efficiency assessment of CTRL vs 29PCM-20: (a) heating-cooling cycles, (b) heating phases and (c) cooling phases.

4 Conclusions

In this work, a bio-based PCM (29PCM) has been successfully incorporated into air lime mortars at 5%, 10% and 20% bwol. This incorporation has been possible thanks to the simultaneous addition of an adhesion booster and a superplasticizer in order to mitigate typical adverse effects of the addition of PCMs. The interactions and compatibilities of the different chemical additives with the bio-based PCM in the lime matrix have been studied. The high compatibility of both the polycarboxylate ether derivative (superplasticizer) and the starch derivative (adhesion booster) with the 29PCM in the lime matrix has been demonstrated. In this way, it has been possible to optimize the formulation of the PCM-bearing mortars always considering their application as renders. This results in mortars that are easy to work with, easy to spread, crack-free and with full adhesion.

With regard to fresh properties, 29PCM-bearing mortars retain characteristics such as percentage of occluded air, fresh mortar density, water retention and setting time very similar to PCM-free mortars. Just consistence increased upon addition of PCM, but the mortar always kept the appropriate fluidity for its final application as a render.

Regarding the characterization of the hardened mortar, its microstructure, mechanical performance and thermal efficiency have been studied. Microstructural studies have revealed homogeneous and continuous materials in which the microencapsulated PCMs are evenly distributed and completely integrated into the lime matrix. Regarding the porous structure, a shift towards a larger pore size distribution was observed following the addition of 29CPM. Particularly noteworthy is the increase in average pore size in the mortar with a higher dose of PCM (20%).

Concerning mechanical performance, a rise in compressive strength was observed when comparing mortars with doses of up to 10% of 29PCM to PCM-free mortar. However, the highest PCM dose (20%) exhibited a deterioration in mechanical performance, likely attributable to the increase in average pore size.

The thermal assessment of the mortars indicated that the addition of 29PCM does not significantly impact thermal conductivity. This could be advantageous as it facilitates heat transfer within the material, enabling PCM to undergo phase changes.

Lastly, thermal efficiency experiments have revealed the ability of the bio-based PCM to store and release heat, thereby attenuating temperatures and considerably improving thermal comfort. 29PCM is therefore postulated as a suitable PCM for improving the energy efficiency of lime mortars in a greener way than conventional PCMs based on paraffins.

References

[1] C. V Podara, I. A. Kartsonakis, and C. A. Charitidis, Towards Phase Change Materials for Thermal Energy Storage: Classification, Improvements and Applications in the Building Sector, Appl. Sci. **11**, 1490 (2021).

[2] R. Naresh, R. Parameshwaran, and V. Vinayaka Ram, Bio-Based Phase-Change Materials (LTD, 2020).

[3] B. P. Jelle and S. E. Kalnaes, Phase Change Materials for Application in Energy-Efficient Buildings, in Cost-Effective Energy Efficient Building Retrofitting (Woodhead Publishing, 2017).

[4] M. Frigione, M. Lettieri, A. Sarcinella, and J. B. de Aguiar, Sustainable Polymer-Based Phase Change Materials for Energy Efficiency in Buildings and Their Application in Aerial Lime Mortars, Constr. Build. Mater. **231**, 117149 (2020).

[5] K. Pielichowska and K. Pielichowski, Phase Change Materials for Thermal Energy Storage, Prog. Mater. Sci. **65**, 67 (2014).

[6] T. de Rubeis, I. Nardi, M. Muttillo, and D. Paoletti, The Restoration of Severely

Damaged Churches – Implications and Opportunities on Cultural Heritage Conservation, Thermal Comfort and Energy Efficiency, J. Cult. Herit. **43**, 186 (2020).

[7] M. Jaradat, H. Al Majali, C. Bendea, C. C. Bungau, and T. Bungau, Enhancing Energy Efficiency in Buildings through PCM Integration: A Study across Different Climatic Regions, BUILDINGS **14**, (2024).

[8] X. N. Chen, B. Xu, X. Xie, and G. Pei, Evaluating and Optimizing the Energy Saving Benefits of Latent Heat in Phase Change Materials with New Indices, Appl. Therm. Eng. **228**, 120479 (2023).

[9] M. Frigione, M. Lettieri, and A. Sarcinella, Phase Change Materials for Energy Efficiency in Buildings and Their Use in Mortars, Materials (Basel). **12**, 1260 (2019).

[10] M. K. Rathod and J. Banerjee, Thermal Stability of Phase Change Materials Used in Latent Heat Energy Storage Systems: A Review, Renew. Sustain. ENERGY Rev. **18**, 246 (2013).

[11] L. Y. Zhang, Q. Z. Zhang, L. W. Jin, X. Cui, and X. H. Yang, Energy, Economic and Environmental (3E) Analysis of Residential Building Walls Enhanced with Phase Change Materials, J. Build. Eng. **84**, (2024).

[12] H. Akeiber, P. Nejat, M. Z. Abd Majid, M. A. Wahid, F. Jomehzadeh, I. Z. Famileh, J. K. Calautit, B. Hughes, and S. A. Zaki, A Review on Phase Change Material (PCM) for Sustainable Passive Cooling in Building Envelopes, Renew. Sustain. ENERGY Rev. **60**, 1470 (2016).

[13] A. Sharma, V. V Tyagi, C. R. Chen, and D. Buddhi, Review on Thermal Energy Storage with Phase Change Materials and Applications, Renew. Sustain. ENERGY Rev. **13**, 318 (2009).

[14] T. W. Fu, W. Z. Wang, and G. Y. Fang, Thermal Properties and Applications of Form-Stable Phase Change Materials for Thermal Energy Storage and Thermal Management: A Review, ENERGY STORAGE **6**, (2024).

[15] M. F. Junaid, Z. ur Rehman, N. Ijaz, R. Farooq, U. Khalid, and Z. Ijaz, Performance Evaluation of Cement-Based Composites Containing Phase Change Materials from Energy Management and Construction Standpoints, Constr. Build. Mater. **416**, 135108 (2024).

[16] G. Li, G. Xu, and J. Zhang, Experimental Investigation of Thermal and Mechanical Characteristics of Slag Cement Mortars with PCM for Radiant Floors, Case Stud. Constr. Mater. **20**, e02958 (2024).

[17] V. Z. Vargas, L. J. Claros-Marfil, G. F. B. Sandoval, B. H. Rojas, A. G. Santos, and F. J. N. González, Experimental Assessment of Energy Storage in Microencapsulated Paraffin PCM Cement Mortars, Case Stud. Constr. Mater. **20**, e02959 (2024).

[18] P. J. Ong et al., Integration of Phase Change Material and Thermal Insulation Material as a Passive Strategy for Building Cooling in the Tropics, Constr. Build. Mater. **386**, (2023).

[19] T. T. Yang, Y. Ding, B. Z. Li, and A. K. Athienitis, A Review of Climate Adaptation of Phase Change Material Incorporated in Building Envelopes for Passive Energy Conservation, Build. Environ. **244**, (2023).

[20] C. H. Liu and X. Yu, Microencapsulation of Biobased Phase Change Material by Interfacial Polycondensation for Thermal Energy Storage Applications, J. BIOBASED Mater. BIOENERGY **7**, 331 (2013).

[21] Z. P. Jaroslav Pokorný, Lucie Zemanová, Milena Pavlíková, Šimon Marušiak, Thermal Properties of Lime-Based Plasters with Expanded Glass Granulate Therm, in AIP Conference Proceedings, Vol. 020015 (AIP Publishing, 2019).

[22] H. Liu, X. Wang, and D. Wu, Innovative Design of Microencapsulated Phase Change Materials for Thermal Energy Storage and Versatile Applications: A Review,

Sustain. Energy Fuels **3**, 1091 (2019).
[23] M. Li, Z. S. Wu, and J. M. Tan, Heat Storage Properties of the Cement Mortar Incorporated with Composite Phase Change Material, Appl. Energy **103**, 393 (2013).
[24] J. G. Speight, Chapter 3 - Hydrocarbons from Petroleum, in edited by J. G. B. T.-H. of I. H. P. Speight (Gulf Professional Publishing, Boston, 2011), pp. 85–126.
[25] I. Asadi, M. H. Baghban, M. Hashemi, N. Izadyar, and B. Sajadi, Phase Change Materials Incorporated into Geopolymer Concrete for Enhancing Energy Efficiency and Sustainability of Buildings: A Review, CASE Stud. Constr. Mater. **17**, e01162 (2022).
[26] European Committee for Standarization, UNE-EN 1015-3 Methods of Test for Mortar for Masonry. Part 3: Determination of Consistence of Fresh Mortar (by Flow Table), EN.
[27] A. Rubio-Aguinaga, J. M. Fernandez, I. Navarro-Blasco, and J. I. Alvarez, Study on the Interaction of Polymeric Chemical Additives with Phase Change Materials in Air Lime Renders, Polymers (Basel). **16**, 1121 (2024).
[28] European Committee for Standarization, UNE-EN 1015-6 Methods of Test for Mortar for Masonry - Part 6: Determination of Bulk Density of Fresh Mortar.
[29] European Committee for Standarization, UNE-EN 1015-7:1999 Methods of Test for Mortar for Masonry. Part 7: Determination of Air Content of Fresh Mortar, EN.
[30] European Committee for Standarization, UNE 83-816-93 Test Methods. Fresh Mortars. Determination of Water Retentivity, EN.
[31] European Committee for Standarization, UNE-EN 1015-9:2000/A1 Methods of Test for Mortar for Masonry. Part 9: Determination of Workable Life and Correction Time of Fresh Mortar, EN.
[32] J. F. Gonzalez-Sanchez, B. Tasci, J. M. Fernandez, I. Navarro-Blasco, and J. I. Alvarez, Combination of Polymeric Superplasticizers, Water Repellents and Pozzolanic Agents to Improve Air Lime-Based Grouts for Historic Masonry Repair, Polymers (Basel). **12**, 887 (2020).
[33] A. Izaguirre, J. Lanas, and J. I. Álvarez, Behaviour of a Starch as a Viscosity Modifier for Aerial Lime-Based Mortars, Carbohydr. Polym. **80**, 222 (2010).
[34] L. Haurie, S. Serrano, M. Bosch, A. I. Fernandez, and L. F. Cabeza, Single Layer Mortars with Microencapsulated PCM: Study of Physical and Thermal Properties, and Fire Behaviour, ENERGY Build. **111**, 393 (2016).
[35] M. Theodoridou, L. Kyriakou, and I. Ioannou, PCM-Enhanced Lime Plasters for Vernacular and Contemporary Architecture, Energy Procedia **97**, 539 (2016).